REPRINT

EUROPTO SERIES

Reprinted from

Earth Surface Remote Sensing II

21, 24 September 1998
Barcelona, Spain

Volume 3496

Laser methods for the atmospheric correction of marine radiance data sensed from satellite

Luca Fiorani, Stefania Mattei, and Sergio Vetrella
CORISTA, Piazzale Tecchio 80, 80125 Naples, Italy

ABSTRACT

Satellite remote sensing of sea color is a powerful instrument to perform oceanic studies. Unfortunately, the present data processing algorithms are not exempt from uncertainties, especially because the marine radiance must be separated from the atmospheric contributions, which typically represent about 80% of the total. In this paper we suggest the development of observation methods based on the optical radar or lidar. In fact, the numerical simulation of a sea-level optical radar demonstrates that, if applied to restricted areas, such system is a precise and versatile tool for the atmospheric correction of marine radiance data sensed from satellite (accuracy better than 10% for typical conditions). Moreover, the lidar is effective even in environments that would be severe for the standard corrective schemes. Finally, the feasibility of a spaceborne system is discussed.

Keywords: ocean color, atmospheric correction, phytoplankton, aerosol, lidar.

1. INTRODUCTION

Satellite observation of the sea color or, more precisely, of the radiance backscattered out by its surface layer at different wavelengths, is one of the more powerful tools for effect large-scale investigations on its properties[1]. In particular, the color of the sea is directly connected to the pigment concentration. This latter, in turn, is linked to the presence of the microorganisms responsible of photosynthesis[2]. For example, the determination of the chlorophyll concentration furnishes an evaluation of the phytoplankton content. The applications of these studies are countless and ranges from the analysis of the pollution effects on the marine ecosystem to the determination of the spatial and temporal distributions of phytoplankton blooms, from the quantification of the relationships between ocean physics and patterns of productivity to the identification of global biogeochemical cycles[3].

The CZCS radiometer (NASA, United States)[4], operational on the Nimbus-7 satellite from 1978 to 1986, has demonstrated the capabilities of space remote sensing of the marine properties. As a result of the CZCS success, the international scientific community has planned a whole series of space missions focused on ocean color observation. Besides MOS (DLR, Germany), OCTS (NASDA, Japan) and SeaWiFS (NASA), launched before the end of 1997, OCI (Taiwan), MODIS (NASA), GLI (NASDA), MERIS (ESA, European Union) and "Low resolution camera" (South Korea) will be launched before 2000.

In general, the pigment concentration is determined with bio-optical algorithms from the measurement of the marine radiance at some wavelengths[5, 6]. Unfortunately, this procedure is not exempt from uncertainties: from one hand the bio-optical algorithms must be fine tuned, on the other hand the marine radiance must be separated from the atmospheric one, that typically represents about 80% of the total radiance measured by the sensor[7]. The final accuracy of C, pigment concentration, is around 30-40% in the best conditions ($0 < C < 1.5$ mg m^{-3} and rather clear atmosphere)[5]. Precise methods for the atmospheric correction, that is for the subtraction of the radiance backscattered from the atmosphere to that measured by the sensor, are essential for an accurate determination of the pigment concentration.

Unfortunately, despite the remarkable success in the ocean observation, the corrective schemes used up to now exhibit some inadequacies, as it has been highlighted by some local studies. In the framework of the SeaWiFS mission and, in particular, of the SYMPLEX (SYnoptic Mesoscale PLankton EXperiment) project, this paper represents a contribution to the development of laser methods for the atmospheric correction, with special emphasis on the analysis of restricted sea regions (channels, gulfs, straits etc.).

After having examined the present algorithms (section 2), a correction method based on the optical radar or lidar is described in section 3. Advantages, drawbacks and suitability of this tool will be discussed in the conclusion (section 4). For a general introduction to the problems and terms of atmospheric optics the reader is referred to one of the available textbooks on the subject[8].

For further information, please contact Luca Fiorani: Email: fiorani@unina.it; Telephone: +39-081-593-9073; Fax: +39-081-593-3576.

Part of the EUROPTO Conference on Remote Sensing of the Ocean and Sea Ice IV
Barcelona, Spain • September 1998
SPIE Vol. 3496 • 0277-786X/98/$10.00

2. PRESENT ALGORITHMS OF ATMOSPHERIC CORRECTION

The present algorithms of atmospheric correction are abundantly described in the literature[5, 6, 9-12]. Here we will treat them briefly, examining their hypotheses and approximations.

The first method consists in comparing satellite data with those obtained in the same sea area by a spectrometer mounted on a ship. In the hypothesis of homogeneous atmosphere, the correction can be extended to the entire image. This scheme, apart from requiring additional observations, presents two remarkable disadvantages. Firstly, the scaling up of the spectrometer resolution to the satellite one (about 1 km × 1 km) should be established with caution. Secondly, the extrapolation of the correction from one point to the whole image may lead to important errors, also in fairly uniform atmospheric conditions. It is not amazing that the pigment concentrations computed with this method differ of around a factor 2 from those measured in situ[5].

There are then the corrective schemes based on atmospheric models. Albeit they do not require additional observations and perform detailed theoretical calculations, they lack of accuracy and are hardly applicable because of the enormous variability of the aerosol content and, consequently, of the optical properties of the real atmosphere[12].

A third type of algorithm is based on the experimental observation that, where the pigment concentration is less than 0.25 mg m^{-3}, the radiance of the sea is constant and known in some spectral bands. Additional observations are not necessary since the regions in which this condition holds ("clear water zones") can be located from satellite because of their low radiance. Because of its undeniable success, this corrective scheme is the most accepted: the remainder of this section will be then devoted to describe it and to discuss its performance[5, 6, 10, 11].

2.1. STANDARD ALGORITHM: DESCRIPTION

Assuming that the remote sensed radiance due to the sun glint (mirror-like reflection of the air-water interface without interaction with the atmosphere) is negligible - thanks to a favorable inclination of the sensor[3] - and that the photons, in their sun-satellite path, undergo only one collision in air (single scattering), the radiance measured by the sensor can be written as:

$$L_t(\lambda) = L_r(\lambda) + L_a(\lambda) + t(\lambda) L_w(\lambda), \tag{1}$$

where L_r is the radiance due to scattering from atmospheric molecules, L_a is the radiance due to scattering from atmospheric aerosols, L_w is the radiance due to scattering from the sea, t is the diffuse transmittance, λ is the wavelength (fig. 1). L_r is computed according to the classical electromagnetic theory (Rayleigh scattering), applicable out of the molecular absorption bands.

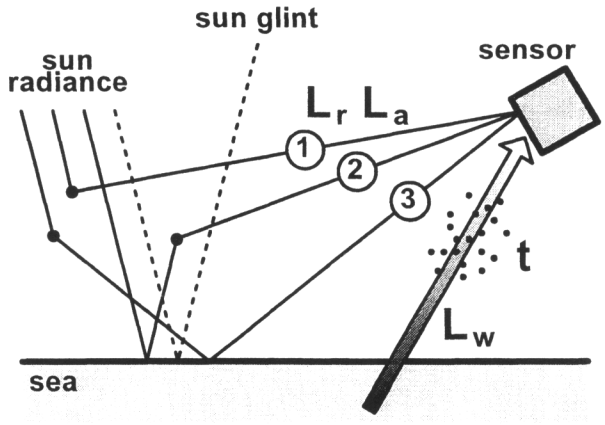

Fig. 1. Illustration of the contributions to the radiance measured by the sensor. The points represent generic atmospheric scatterers (molecules, aerosols).

The task of the corrective algorithm is to retrieve the value of L_w from the measurement of L_t, that is to determine L_r, L_a and t. L_r and L_a include the atmospheric single scattering (path 1 in fig. 1) and the mirror-like reflection of the air-water interface before or after the atmospheric scattering (path 2 or 3 in fig. 1, respectively). As a consequence, L_w does not cover the reflection of the air-water interface. The diffuse transmittance has been used rather than the direct transmittance because part of the radiance measured by the sensor is emitted from regions adjacent to those observed.

Adopting the convention that the subscript x could be r as well as a, L_r and L_a can be expressed as follows:

$$L_x(\lambda) = \frac{\omega_x(\lambda)\,\tau_x(\lambda)\,F_0'(\lambda)\,p_x(\theta_0,\theta,\lambda)}{4\pi}, \tag{2}$$

$$F_0'(\lambda) = F_0(\lambda)\exp\left[-\tau_{O_3}(\lambda)\left(\frac{1}{\cos\theta_0}+\frac{1}{\cos\theta}\right)\right], \tag{3}$$

$$p_x(\theta_0,\theta,\lambda) = \frac{P_x(\theta_-,\lambda)+[\rho(\theta_0,\lambda)+\rho(\theta,\lambda)]P_x(\theta_+,\lambda)}{\cos\theta}, \tag{4}$$

$$\cos\theta_\pm = \pm\cos\theta_0\cos\theta + sin\theta_0 sin\theta\cos(\phi_0-\phi), \tag{5}$$

where ω_x is the albedo, τ_x is the optical thickness, F_0 is the instantaneous extraterrestrial solar irradiance, τ_{O_3} is the ozone optical thickness, θ_0 and θ are the zenith angles of the sun and of the sensor, respectively, P_x is the phase function, ρ is the reflectance of the air-water interface, ϕ_0 and ϕ are the azimuth angles of the sun and of the sensor, respectively.

Concerning the diffuse transmittance, we can write:

$$t(\lambda) = \exp\left[-\frac{\frac{\tau_r(\lambda)}{2}+\tau_{O_3}(\lambda)}{\cos\theta}\right]t_a(\lambda), \tag{6}$$

$$t_a(\lambda) = \exp\left\{-\frac{[1-\omega_a(\lambda)\psi(\lambda)]\tau_a(\lambda)}{\cos\theta}\right\}, \tag{7}$$

where ψ is the probability that a photon will be forward scattered (scattering angle less than 90°).

In case the photons, in their sun-satellite path, undergo more than one collision in air (multiple scattering), equations (1) and (2) are not exact. Detailed calculations demonstrate that, while the first remains substantially valid, the second furnishes a poor estimate of L_a. Moreover, we point out that relationship (4) has been obtained assuming that the sea surface is flat. If this is not true, each ρP_x term becomes the integral over the solid angle of essentially the product of ρP_x and the surface slope probability density function[13].

The terms concerning molecular scattering, the instantaneous extraterrestrial solar irradiance and the ozone optical thickness can be modeled very precisely, thanks to the regularity of the phenomena determining them. More troublesome is the problem of the terms linked to the aerosols, because of the high variability of their constitution and concentration.

The standard algorithm eludes this problem by means of the radiance measurement at 4 wavelengths (λ_1, λ_2, λ_3 and λ_4 that, for CZCS, are 443, 520, 550 and 670 nm, respectively) and of a transformation of equation (1):

$$L_w(\lambda_i) = \frac{L_t(\lambda_i)-L_r(\lambda_i)-S(\lambda_i,\lambda_4)[L_t(\lambda_4)-L_r(\lambda_4)-t(\lambda_4)L_w(\lambda_4)]}{t(\lambda_i)} \qquad i=1,2,3\,. \tag{8}$$

The three relationships (8) contain 11 unknown:

$$L_w(\lambda_j) \qquad j = 1,2,3,4\,, \tag{9}$$

$$S(\lambda_i,\lambda_4) \equiv \frac{L_a(\lambda_i)}{L_a(\lambda_4)} \qquad i = 1,2,3\,, \tag{10}$$

$$t(\lambda_j) \qquad j = 1,2,3,4\,. \tag{11}$$

but the problem has been solved estimating S, t and adding one more equation:

$$f[L_w(\lambda_1), L_w(\lambda_3), L_w(\lambda_4)] = 0\,, \tag{12}$$

where f is an empirical function. The evaluation of t has been obtained assuming simply:

$$t_a(\lambda_j) = 1 \qquad j = 1,2,3,4\,. \tag{13}$$

This latter hypothesis is justified from the fact that - according to the models - the factor $(1-\omega_a\psi)$ of formula (7) is always less than 1/6.

Concerning the evaluation of S, the algorithm is based on the concept of clear water zones, that is on the experimental observation that $L_w(\lambda_2)$, $L_w(\lambda_3)$ and $L_w(\lambda_4)$ are constant and known where the pigment concentration is less than 0.25 mg m^{-3}. At first, thanks to its low radiance, one locates from satellite a portion of sea in which this condition holds ("calibration region"). Then, from the known values of $L_w(\lambda_2)$, $L_w(\lambda_3)$ and $L_w(\lambda_4)$, $S(\lambda_2,\lambda_4)$ and $S(\lambda_3,\lambda_4)$ are obtained through relationship (8). The determination of $S(\lambda_1,\lambda_4)$ it is a little more complex and it is based on the observation that S obeys approximately the following law:

$$S(\lambda_i,\lambda_4) = \left(\frac{\lambda_i}{\lambda_4}\right)^{n(\lambda_i)} \qquad i = 1,2,3\,, \tag{14}$$

and then $n(\lambda_2)$ and $n(\lambda_3)$ could be calculated from $S(\lambda_2,\lambda_4)$ and $S(\lambda_3,\lambda_4)$. Finally, the simple hypothesis:

$$n(\lambda_1) = \frac{n(\lambda_2) + n(\lambda_3)}{2}\,, \tag{15}$$

can be used to compute $S(\lambda_1,\lambda_4)$ from formula (14).

Up to now we have calculated the atmospheric correction in the calibration region. At this point we should solve the problem of extrapolating the values of S just found to the entire remote sensed image. At first we observe that, from equations (2) and (10), we can write:

$$S(\lambda_i,\lambda_4) = \varepsilon(\lambda_i,\lambda_4)\frac{F_0'(\lambda_i)}{F_0'(\lambda_4)} \qquad i = 1,2,3\,, \tag{16}$$

$$\varepsilon(\lambda_i,\lambda_4) \equiv \frac{\omega_a(\lambda_i)\tau_a(\lambda_i)p_a(\theta_0,\theta,\lambda_i)}{\omega_a(\lambda_4)\tau_a(\lambda_4)p_a(\theta_0,\theta,\lambda_4)} \qquad i = 1,2,3\,, \tag{17}$$

and so the determination of S is replaced by that of ε. In addition, the aerosol models indicate that ω_a and p_a are weak functions of λ, then we can write:

$$\varepsilon(\lambda_i,\lambda_4) \cong \frac{\tau_a(\lambda_i)}{\tau_a(\lambda_4)} \qquad i = 1,2,3\,. \tag{18}$$

This latter relationship is approximately valid also in case of multiple scattering. Finally, assuming that the aerosols are of the same kind (size distribution and refractive index both constant), it has been shown that the $\tau_a(\lambda_i)/\tau_a(\lambda_4)$ ratio can be extrapolated to all the image, even in presence of inhomogeneous aerosol concentration.

2.2. STANDARD ALGORITHM: DISCUSSION

The authors of the standard algorithm have determined its performance and recognized its limitations: in the following we will summarize briefly the results of their studies.

1) The algorithm achieves an accuracy of about 10-20% in the determination of L_w.

2) The algorithm is applicable to rather clear atmospheres (optical thickness less than 0.1), that is when the single scattering hypothesis holds (the comparison between ship and satellite measurements shows an important discrepancy in case of haze).

3) In presence of horizontally inhomogeneous aerosols - a possible case in coastal zones[14] - the algorithm is effective only in three cases:

   a) if the pigment concentration is low (each pixel of the image can be used as calibration region),

   b) if there are two kinds of aerosols and a clear water zone can be located under the region of more turbid atmosphere (errors in L_w of about 20%),

   c) if there are two kinds of aerosols and a clear water zone can not be located under the region of more turbid atmosphere (errors in L_w fairly high).

4) The accuracy of the algorithm considerably degrades if multiple scattering has to be taken into account, even in presence of only one kind of aerosols (ε constant). Gordon *et al.*[5] carry out an exemplar calculus: extrapolating the value of ε from a calibration region where the optical thickness is 0.1 (λ_1) to portions of image where the optical thickness is 0.2 and 0.4, they obtain errors in L_w of 15% and 100%, respectively. Moreover, if one admits that ε might change of 10% the uncertainties become totally unacceptable.

5) The algorithm fails if the absolute radiometer calibration is not precise. Gordon *et al.*[5] show that, if the sensor yields radiances that are 5% too high in the blue, negative values of L_w are obtained out of the calibration region in presence of horizontally inhomogeneous aerosols. In order to circumvent this problem, they suggest to multiply the radiometer calibration times a corrective factor. This latter is adjusted by trial and error, requiring that ε is stable during successive satellite passes in the clear water zones.

6) If various clear water zones are present in an image, different values of ε are found, even if the atmosphere is not turbid. Gordon *et al.*[5] recommend to choose as calibration region the clear water zone where $L_a(\lambda_4)$ is maximum and the series $L_a(\lambda_2)$, $L_a(\lambda_3)$, $L_a(\lambda_4)$ is monotonic.

7) The algorithm accuracy is linked to the pigment concentration in the calibration region. This effect is important in the portions of sea with high pigment concentration or, at worst, with suspended sediments (coastal zones). Gordon *et al.*[5] suggest to choose as calibration region the clear water zone where the pigment concentration is minimum. Nevertheless, the observation of the seasonal pigment change could be altered by the temporal evolution of their concentration in the calibration region. This phenomenon could explain the anomalies found in some studies of the Mediterranean Sea[15].

8) The known values of L_w, used for the determination of S in the calibration region, are the result of measurement campaigns close to US: studies conducted in other geographical zones have highlighted the algorithm failure[16].

In conclusion, we can affirm that the standard algorithm is put to trial in presence of horizontally inhomogeneous aerosols and of high pigment concentrations or suspended sediments. All those conditions tend to occur beside the coasts. The key for a substantial improvement of the atmospheric correction is an accurate determination of ε in each pixel of the remote sensed image. In the following section we will suggest an algorithm particularly suitable for coastal zones (channels, gulfs, straits etc.) since it is based on a direct measurement of ε.

3. TOWARD MORE RELIABLE ATMOSPHERIC CORRECTION ALGORITHMS

As we have seen in the preceding section, an accurate determination of ε is necessary in order to obtain a precise correction of marine radiance data. According to relationship (18) - approximately valid also in case of multiple scattering - ε can be computed from τ_a (aerosol optical thickness). Although this variable can be measured quickly by the optical radar and such measurements have been compared in the past with the values predicted by atmospheric models[12], only recently it has been suggested to use a lidar for the correction of satellite data[17]. In this context, after an introduction to the optical radar, the present work examines the feasibility of both a sea-level and a spaceborne system.

The acronym "lidar" (LIght Detection And Ranging) has been introduced in analogy with "radar" in the context of the pulsed light detectors of clouds[18]. Albeit this term has been suggested well before the discovery of the laser (conceived by Schawlow and Townes in December 1958 and realized by Maiman in July 1960)[19], only with its advent the lidar has spread.

The new capabilities offered to the atmospheric studies by this revolutionary source of light have been soon understood and exploited[20-23]. Because of its characteristics (high intensity, small divergence, short pulse duration and excellent monochromaticity) the laser beam is the ideal tool for active optical remote sensing. The measurement, up to many kilometers of height, of density, temperature and humidity of air, the detection of trace gases, the study of clouds, the observation of stratospheric aerosols, the probing of high atmosphere and the monitoring of pollutants are some examples among the possible applications of lidar[24-27].

A lidar is essentially composed of a transmitter (laser) and a receiver (telescope). Its principle of operation is illustrated in fig. 2: the backscatterers (molecules, aerosols) at the distance R from the system send back part of the laser pulse toward A, active surface of the telescope. Consequently, the analysis of the detected signal as a function of t, time interval between emission and detection, allows one to study the optical properties of the atmosphere along the beam, since the simple relationship between t and R is given by:

$$R = \frac{ct}{2}, \tag{19}$$

where c is the speed of light.

The photons detected within τ_D, detector response time, are backscattered from the layer delimited by the distances R and $R+c\tau_D/2$. Their number n is proportional to the thickness $c\tau_D/2$ and to the backscattering coefficient β of the involved air volume. Furthermore, in its round trip, the original pulse consisting of n_0 photons is attenuated by the atmosphere. This phenomenon is quantified by the extinction coefficient α. Moreover, n is proportional to the solid angle A/R^2 and the efficiency ζ of the detection system.

On the basis of the preceding discussion, the lidar equation can be finally written[25]:

$$n(R,\lambda) = n_0(\lambda)\zeta(\lambda)\frac{A}{R^2}\beta(R,\lambda)\frac{c\tau_D}{2}\exp\left[-2\int_0^R \alpha(R',\lambda)dR'\right]. \tag{20}$$

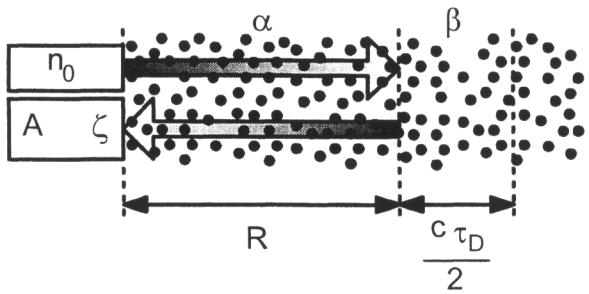

Fig. 2. Lidar principle of operation. The points represent generic atmospheric scatterers (molecules, aerosols).

Once recognized that the integral in equation (20) is just the atmospheric optical thickness between 0 and R, it is clear that a lidar measurement allows one to determine it. Actually α and β are both unknown, but some reliable methods have been elaborated to retrieve them from the signal, on the basis of some reasonable hypothesis[28-31]. In the following we will describe a scheme accepted by many researchers[32].

As we have observed, at first glance equation (20) contains only 2 unknown quantities: α and β. Moreover, it is often very difficult to establish precisely the efficiency of the system. Consequently, the retrieval of α and β requires not only to establish a relationship between them, but also to estimate a constant. As we will see, this latter evaluation will be replaced by the determination of the backscattering coefficient at a given distance.

In order to establish a relationship between the extinction and backscattering coefficients, we distinguish the contributions of molecules and aerosols:

$$\alpha(R,\lambda)=\alpha_r(R,\lambda)+\alpha_a(R,\lambda), \tag{21}$$

$$\beta(R,\lambda)=\beta_r(R,\lambda)+\beta_a(R,\lambda), \tag{22}$$

and we remember that the terms concerning molecular scattering (α_r and β_r) can be modeled very precisely. Finally, we recognize that α_a and β_a are linked by the phase function P_π according to the equation:

$$\alpha_a(R,\lambda)=\frac{1}{P_\pi(R,\lambda)}\beta_a(R,\lambda). \tag{23}$$

Albeit the phase function varies with distance and time, in practice the final result is rather accurate even considering a constant P_π. The P_π value can be selected among those tabulated in the literature according to the aerosol kind (urban, rural, maritime etc.).

After the definition[30]:

$$\mu(R,\lambda)\equiv\ln\left[n(R,\lambda)R^2\right]-2\int_R^{R_M}\left\{\left[1-\frac{3}{8\pi P_\pi(R',\lambda)}\right]\alpha_r(R',\lambda)\right\}dR', \tag{24}$$

where R_M is a given distance, the following differential equation is obtained from relationships (20) - (24):

$$\frac{d\mu(R,\lambda)}{dR}=\frac{1}{\beta(R,\lambda)}\frac{d\beta(R,\lambda)}{dR}-\frac{2}{P_\pi(R,\lambda)}\beta(R,\lambda), \tag{25}$$

whose solution is[28]:

$$\beta(R,\lambda)=\frac{\exp[\mu(R,\lambda)-\mu_M(\lambda)]}{\frac{1}{\beta_M(\lambda)}+\frac{2}{P_\pi(R,\lambda)}\int_R^{R_M}\exp[\mu(R',\lambda)-\mu_M(\lambda)]dR'}, \tag{26}$$

$$\mu_M(\lambda)\equiv\mu(R_M,\lambda), \tag{27}$$

where β_M is the integration constant. Finally, from relationships (21) - (23), we obtain the extinction coefficient and therefore the optical thickness. Solution (26) has been formulated so that β_M is equal to $\beta(R_M)$. If a large R_M is chosen (corresponding to the free troposphere), the aerosol contribution to the backscattering coefficient is negligible and then β_M can be computed very precisely.

The analysis of the accuracy in the optical thickness measurement is rather complex: we will summarize here only the main results, referring the reader to a specific study[33] for a more complete treatment.

The statistical relative error of α is about equal to that of the lidar signal. This latter can be approximately written as[34, 35]:

$$s_n = \sqrt{n + n_B + n_D}\ , \tag{28}$$

where n_B and n_D are the number of photon counts calculations originated by the brightness of the sky (solar background) and the electronic noise of the detector (dark current), respectively. Finally, the statistical uncertainty of ε is obtained applying the error propagation formula.

The systematic error of α is dominated by the imprecise choice of P_π and it is of the order of 10%. However, this uncertainty has a very small effect in the determination of ε since, according to formula (18), it is given by the ratio of optical thicknesses.

3.1. SEA-LEVEL LIDAR

In this section we describe a lidar (fig. 3) conceived for the atmospheric correction of marine radiance data on local scale (channels, gulfs, straits etc.). It could be realized with commercial components and would be compact enough to be transported by truck or ship.

The transmitter is based on a Nd:YAG laser with second and third harmonic generators (beams at 355, 532 and 1064 nm). This source covers the spectral region from UV to IR and has the advantage of being reliable and user-friendly. The receiver consists of a reflector telescope for light collection, of dielectric mirrors and interference filters for wavelength selection and of photomultiplier tubes for photon detection. The characteristics of the components listed in table 1 are closely inspired to those of commercial models.

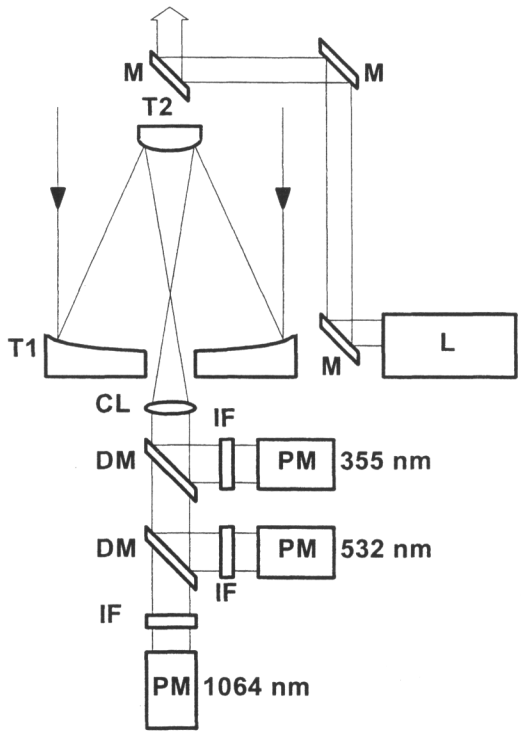

Fig. 3. Outline of a lidar conceived for the atmospheric correction of marine radiance data. L: laser, M: mirror, T1: telescope primary mirror, T2: telescope secondary mirror, CL: collimating lens, DM: dielectric mirror, IF: interference filter, PM: photomultiplier tube.

	355 nm	532 nm	1064 nm
Pulse energy [mJ]	200	200	400
Optical efficiency (transmitter and receiver) [%]	50	50	50
Photomultiplier quantum efficiency [%]	25	10	0.08
Filter transmittance [%]	30	40	50
Filter bandwidth [nm]	0.3	0.3	0.5
Photomultiplier dark current [counts per second]	10	10	7000
Telescope diameter [cm]	50		

Table 1. Characteristics of a lidar conceived for the atmospheric correction of marine radiance data.

The system sweeps the whole hemisphere providing a fast and accurate measurement of ε in an atmospheric column having a diameter of many km, as shown in fig. 4. The lidar can be aimed in various ways: either rotating together the transmitter-receiver couple[36] or directing their optical axes by means of a pair of plain mirrors (like in an astronomic solar observatory)[37]. A realistic measurement cycle involve a series of determinations in different directions (azimuth and zenith angle step of the order of 15°). The data are then interpolated to retrieve the atmospheric optical thickness above the points of the surface whose distance from the lidar is less than a "measurement radius" (fig. 4). The spatial resolution is about 1 km, the temporal one 100 - 1000 s, depending on laser repetition rate (typically 10 - 100 Hz) and actuators speed.

The statistical error for this lidar has been evaluated with a numerical simulation of signal and noise based on standard models of atmosphere[38], aerosols[39] and radiance[40]. Concerning the solar background we have put ourselves in the worst condition (telescope aimed toward the sun). The final results have been listed in table 2, as a function of measurement radius and wavelength. In the UV, the error becomes unacceptable beyond 15 km because of the large atmospheric absorption. Table 2 gives only an estimate since the actual system performance depends on the real aerosol content.

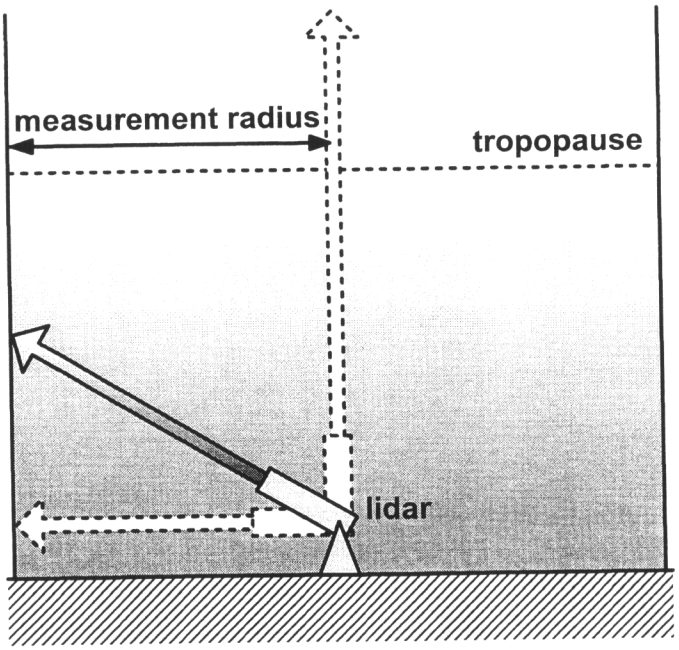

Fig. 4. Optical thickness measurement in an atmospheric column by means of a lidar able to sweep the whole hemisphere.

	355 nm	532 nm	1064 nm
5 km	0.02	0.03	0.3
10 km	0.1	0.1	1
15 km	4	0.7	2
20 km	200	6	5
25 km		50	20

Table 2. Statistical error of the optical thickness [%] as a function of measurement radius and wavelength for the lidar whose characteristics are listed in table 1 (numerical simulation).

The reader has certainly observed that the lidar suggested here measures the optical thickness at three wavelengths (355, 532 and 1064 nm) different from those detected by the sensor (λ_1, λ_2, λ_3 and λ_4). The problem is then to calculate the optical thicknesses $\tau(\lambda_1)$, $\tau(\lambda_2)$, $\tau(\lambda_3)$ and $\tau(\lambda_4)$ from the measurements $\tau(355)$, $\tau(532)$ and $\tau(1064)$. Fortunately, the optical thickness obeys in good approximation to the following law[25]:

$$\tau_a(\lambda) = \frac{a}{\lambda^b}, \tag{29}$$

whose coefficients a and b can be determined by fit to the experimental data.

In conclusion, taking into account the optical thickness error, we can affirm that a simple and compact lidar is able of determine ε, and then L_W, with an accuracy better than 10% in a 30 km wide atmospheric column (with spatial and temporal resolution of about 1 km and 100-1000 s, respectively). Moreover, the lidar has an important advantage: it can furnish the atmospheric correction to marine radiance data even in conditions that would be severe, if not prohibitive, for the standard algorithm described in section 2.1 (for example, for optical thickness higher than 0.1, pigment concentration stronger than 1.5 mg m^{-3} and in presence of horizontally inhomogeneous aerosols).

3.2. SPACEBORNE LIDAR

The more elegant solution to the problem of the atmospheric correction of marine radiance data would be to mount the lidar on the satellite exploiting the receiving optics already existing in the sensor. In this case an additional sea-level system would not be necessary and the whole remote sensed image would be corrected.

After the success of LITE (Lidar In-space Technology Experiment)[41], in which an optical radar has been mounted on the Space Shuttle, the spaceborne lidar has become a reality, even if it remains a technological challenge. Considering the lidar described above and imagining to put it in an orbit at 200 km of height, the numerical simulation points out that the optical thickness of the atmospheric column under it could be determined with a precision better than 10%, averaging over 100 pulses (corresponding to a laser operation time between 1 and 10 s).

More ambitious is the project of incorporating a miniaturized lidar in a sensor like the SeaWiFS. Unfortunately, even if one imagine to use one of the best available sources (the microchip laser developed recently by the French laboratory CEA/LETI that supplies 3 μJ at 1064 nm and 25 kHz repetition rate) and to average the signal over hours of operation, the numerical simulation forces us to conclude that the measurement of the optical thickness is impossible from a satellite that flies at more than 700 km of height. At the current state of the technology, even the modulation of a continuous wave laser[42] would not provide a sufficient increase of the emitted power. A possible way out could be the observation of the beam reflection by the sea surface but, in order to obtain significant data, it would be necessary to know the reflectance of the air-water interface that, unfortunately, depends on the substances dissolved in the sea and on the ripple of its surface.

4. CONCLUSION

The numerical simulation of an optical radar, developed in the framework of the present paper, demonstrates that such system is a powerful and versatile tool for the atmospheric correction of marine radiance data sensed from satellite. Its main advantage is to overcome, at least locally, all the limitations of the standard algorithm discussed in section 2.2. As a matter of fact, the lidar is effective also in conditions in which usual methods fail, that is:

- for strong marine pigment concentration,

- for high atmospheric optical thickness,

- if different kinds of aerosols are present in the measurement zone.

For typical atmospheric conditions, the final accuracy of the marine radiance determination is better than 10%, in a circle having a diameter of 30 km (with spatial and temporal resolution of about 1 km and 100-1000 s, respectively). Although the extrapolation to the whole image of the correction obtained with the optical radar has the same uncertainties of that effected within the standard algorithm, it is evident that a precise knowledge of the correction - even in a restricted area - is a big advantage. Another merit of the system presented here is the feasibility in a simple and compact configuration, suitable for the installation on mobile platform (truck, ship).

In conclusion, we can affirm that the optical radar is the ideal tool for the precise analysis of restricted sea regions and especially of the coastal zones (channels, gulfs, straits etc.), where pigment concentration is usually larger and inhomogeneous aerosols can easily develop. The direct measurement of the atmospheric correction for the whole remote sensed image would require mounting the lidar on a satellite but, at the present state of the technology, this solution is practicable only at low altitudes (Space Shuttle).

5. ACKNOWLEDGEMENTS

This work was supported by the Italian Space Agency under Contract ARS/CI/97/13.

6. REFERENCES

1. T. D. Allan, "The marine environment", Int. J. Remote Sensing **13**, pp. 1261-1276, 1992.
2. J. Fischer and U. Kronfeld, "Sun-stimulated chlorophyll fluorescence", Int. J. Remote Sensing **11**, pp. 2125-2147, 1990.
3. S. B. Hooker, W. E. Esaias, G. C. Feldman, W. W. Gregg, and C. R. McClain "An overview of SeaWiFS and ocean color", in *SeaWiFS Technical Report Series – Technical Memorandum 104566*, S. B. Hooker and E. R. Firestone, eds., NASA, Washington, US, vol. 1, 1992.
4. W. L. Barnes, "Visible and infrared imaging radiometers for ocean observations", in *Applications of Remote Sensing to Ocean Surveillance – Lecture Series 88*, AGARD-NATO, Neuilly sur Seine, France, pp. 7.1-7.20, 1977.
5. H. R. Gordon, D. K. Clark, J. W. Brown, O. B. Brown, R. H. Evans, and W. W. Broenkow, "Phytoplankton pigment concentrations in the Middle Atlantic Bight: comparison of ship determinations and CZCS estimates", Appl. Opt. **22**, pp. 20-36, 1983.
6. J.-M. André and A. Morel, "Atmospheric corrections and interpretation of marine radiances in CZCS imagery, revisited", Oceanol. Acta **14**, pp. 3-22, 1991.
7. H. R. Gordon, "Removal of atmospheric effects from satellite imagery of the oceans", Appl. Opt. **17**, pp. 1631-1636, 1978.
8. E. J. McCartney, *Optics of the Atmosphere*, Wiley, New York, US, 1976.
9. H. R. Gordon and A. Morel, *Remote Assessment of Ocean Color for Interpretation of Satellite Visible Imagery. A Review*, Springer, Heidelberg, Germany, 1983.
10. H. R. Gordon and D. K. Clark, "Clear water radiances for atmospheric correction of coastal zone color scanner imagery", Appl. Opt. **20**, pp. 4175-4180, 1981.
11. R. C. Smith and W. H. Wilson, "Bio-optical research in the Southern California Bight", in *Oceanography from Space*, J. F. R. Gower, ed., Plenum, New York, US, pp. 281-294, 1981.
12. S. Mukai, "Atmospheric correction of remote sensing images of the ocean based on multiple scattering calculations", IEEE Trans. Geosci. Remote Sensing **28**, pp. 696-702, 1990.
13. C. Cox and W. Munk, "Measurement of the roughness of the sea surface from photographs of the sun glitter", J. Opt. Soc. Am. **44**, pp. 838-850, 1954.

14. E. Durieux, L. Fiorani, B. Calpini, M. Flamm, L. Jaquet, and H. Van den Bergh, "Tropospheric ozone measurements over the Great Athens Area during the MEDCAPHOT-TRACE campaign with a new shot-per-shot DIAL instrument. Experimental system and results", Atmos. Environ. **32**, pp. 2141-2150, 1998.
15. M. Ribera, Private communication, 1997.
16. M. Toratani and H. Fukushima, "Atmospheric correction scheme for ocean color remote sensing in consideration to Asian dust aerosol", in *Proc. of the IGARSS 3*, IEEE, Piscataway, US, pp. 1937-1940, 1993.
17. N. Takeuchi, H. Kuze, Y. Sakurada, T. Takamura, S. Murata, K. Abe, and S. Moody, "Construction of a multi-wavelength lidar system for satellite data atmospheric correction", in *Advances in Atmospheric Remote Sensing with Lidar*, A. Ansmann, R. Neuber, P. Rairoux, and U. Wandinger, eds., Springer, Heidelberg, Germany, pp. 71-74, 1997.
18. W. E. K. Middleton and A. F. Spilhaus, *Meteorological Instruments*, University of Toronto, Toronto, Canada, 1953.
19. J. Hecht, *Laser Pioneers*, Academic, San Diego, US, 1985.
20. G. Fiocco and L. D. Smullin, "Detection of scattering layers in the upper atmosphere by optical radar", Nature **199**, pp. 1275-1276, 1963.
21. G. G. Goyer and R. Watson, "The laser and its application to meteorology", Bull. Am. Meteorol. Soc. **44**, pp. 564-570, 1963.
22. R. T. H. Collis, "Lidar: a new atmospheric probe", Q. J. R. Meteorol. Soc. **92**, pp. 220-230, 1966.
23. V. E. Derr and C. G. Little, "A comparison of remote sensing of the clear atmosphere by optical, radio, and acoustic radar techniques", Appl. Opt. **9**, pp. 1976-1991, 1970.
24. R. T. H. Collis and P. B. Russel, "Lidar measurement of particles and gases by elastic backscattering and differential absorption", in *Laser Monitoring of the Atmosphere*, E. D. Hinkley, ed., Springer, Heidelberg, Germany, pp. 71-151, 1976.
25. R. M. Measures, *Laser Remote Sensing*, Krieger, Malabar, US, 1992.
26. S. F. Clifford, J.C. Kaimal, R. J. Lataitis, and R. G. Strauch, "Ground-based remote profiling in atmospheric studies: an overview", Proc. IEEE **82**, pp. 313-355, 1994.
27. W. B. Grant, "Lidar for atmospheric and hydrospheric studies", in *Tunable Laser Applications*, F. J. Duarte, ed., Dekker, New York, US, pp. 213-305, 1995.
28. J. D. Klett, "Stable analytical inversion solution for processing lidar returns", Appl. Opt. **20**, pp. 211-220, 1981.
29. F. G. Fernald, "Analysis of atmospheric lidar observations: some comments", Appl. Opt. **23**, pp. 652-653, 1984.
30. E. V. Browell, S. Ismail, and S. T. Shipley, "Ultraviolet DIAL measurements of O_3 profiles in region of spatially inhomogeneous aerosols", Appl. Opt. **24**, pp. 2827-2836, 1985.
31. W. Krichbaumer and C. Werner, "Current state-of-the-art of lidar inversion methods for atmospheres of arbitrary optical density", Appl. Phys. B **59**, pp. 517-523, 1994.
32. E. Durieux and L. Fiorani, "Data Processing", in *Instrument Development for Atmospheric Research and Monitoring*, J. Bösenberg, D. Brassington, and P. C. Simon, eds., Springer, Heidelberg, Germany, pp. 89-116, 1997.
33. L. Fiorani, *Une Première Mesure Lidar Combinée d'Ozone et de Vent, à partir d'une Instrumentation et d'une Méthodologie Coup par Coup – PhD Thesis 1585*, EPFL, Lausanne, Switzerland, 1996 (in French).
34. R. M. Schotland, "Errors in the lidar measurements of atmospheric gases by differential absorption", J. Appl. Meteor. **13**, pp. 71-77, 1974.
35. J. Pelon and G. Mégie, "Ozone monitoring in the troposphere and lower stratosphere: evaluation and operation of a ground-based lidar station", J. Geophys. Res. **87**, pp. 4947-4955, 1982.
36. L. Fiorani, B. Calpini, L. Jaquet, H. Van den Bergh, and E. Durieux, "A combined determination of wind velocities and ozone concentrations for a first measurement of ozone fluxes with a DIAL instrument during the MEDCAPHOT-TRACE campaign", Atmos. Environ. **32**, pp. 2151-2159, 1998.
37. R. Velotta, L. Fiorani, P. Di Girolamo, and N. Spinelli, "Compact optical systems for the three-dimensional monitoring of the atmosphere", in *Proc. del Congresso Nazionale di Fisica della Materia*, INFM, Genoa, Italy, p. I/4, 1997.
38. *US Standard Atmosphere*, US Government Printing Office, Washington, US, 1976.
39. L. Elterman, *UV, Visible and IR Attenuation for Altitudes to 50 km – AFCRL-68-0153*, USAF, Hanscom, US, 1968.
40. F. X. Kneizys, G. P. Anderson, E. P. Shettle, W. O. Gallery, L. W. Abreu, J. E. A. Selby, J. H. Chetwynd, and S. A. Clough, *Users Guide to LOWTRAN 7 – AFGL-TR-88-0177*, USAF, Hanscom, US, 1988.
41. D. M. Winker, R. H. Couch, and M. P. McCormick, "An overview of LITE: NASA's lidar in-space technology experiment", Proc. IEEE **84**, pp. 164-180, 1996.
42. V. Mitev, R. Matthey, and D. Reusser, "Development of a pseudorandom noise modulation, continuous-wave (PRN-cw) total backscatter lidar", Proc. SPIE **2505**, pp. 150-160, 1995.